From Darkness to Light
ASP Conference Series, Vol. 243, 2001
T. Montmerle & Ph. André, eds.

Kinematics of Millimeter Prestellar Condensations in the ρ Ophiuchi Protocluster

Arnaud Belloche

CEA Saclay, Service d'Astrophysique, DSM/DAPNIA/SAp, F-91191 Gif-sur-Yvette, France

Philippe André

CEA Saclay, Service d'Astrophysique, DSM/DAPNIA/SAp, F-91191 Gif-sur-Yvette, France

Frédérique Motte

Max-Planck-Institut für Radioastronomie, 53121 Bonn, Germany

Abstract. We analyze the kinematics of the pre-stellar condensations previously identified in an extensive millimeter dust continuum mapping of the ρ Ophiuchi protocluster. Our follow-up line observations confirm that these condensations are gravitationally bound. In addition, the small amplitude of the relative motions we measure indicates that the condensations do not have time to orbit significantly through the gas during their lifetimes. Finally, the spectral signature of collapse and peculiar velocity gradients seen within several pre-stellar condensations suggest that the dynamical phase of isothermal collapse preceding the main accretion stage is very significant in star-forming clusters.
Keywords: ISM: Kinematics, Dynamics, Molecules - Cores: Pre-stellar, Infall, Rotation - Star Formation: Clusters - Clusters: Dynamics, Protoclusters - Stars: Formation - Regions: ρ Oph - Instruments: IRAM-30m

1. Introduction

Using the MPIfR bolometer array on the IRAM 30 m telescope, Motte, André, & Neri (1998a - hereafter MAN98) completed an extensive 1.3 mm continuum mapping survey of the ρ Ophiuchi main cloud, the nearest example of a star-forming cluster ($d \sim 150$ pc). Their 1.3 mm mosaic (see e.g. Fig. 1) provides a census of $\sim 2\,000-4\,500$ AU dust structures in ρ Oph, which should be essentially complete down to a mass sensitivity limit of $\lesssim 0.1$ $M_\odot$. In the angular size-scale range of $15'' - 30''$, a total of 100 fragments were detected, which consist of 41 circumstellar envelopes/disks around embedded young stellar objects and 59 starless condensations undetected by ISOCAM in the mid-IR (cf. Bontemps et al. 2001 - See also Kaas & Bontemps, this volume).

As pointed out by MAN98 (see also André et al. 1999), the mass spectrum of these condensations is remarkable in that it resembles the stellar Initial Mass Function (IMF). The ρ Oph 1.3 mm condensations are thus of great interest to try and better understand the formation process of star clusters.

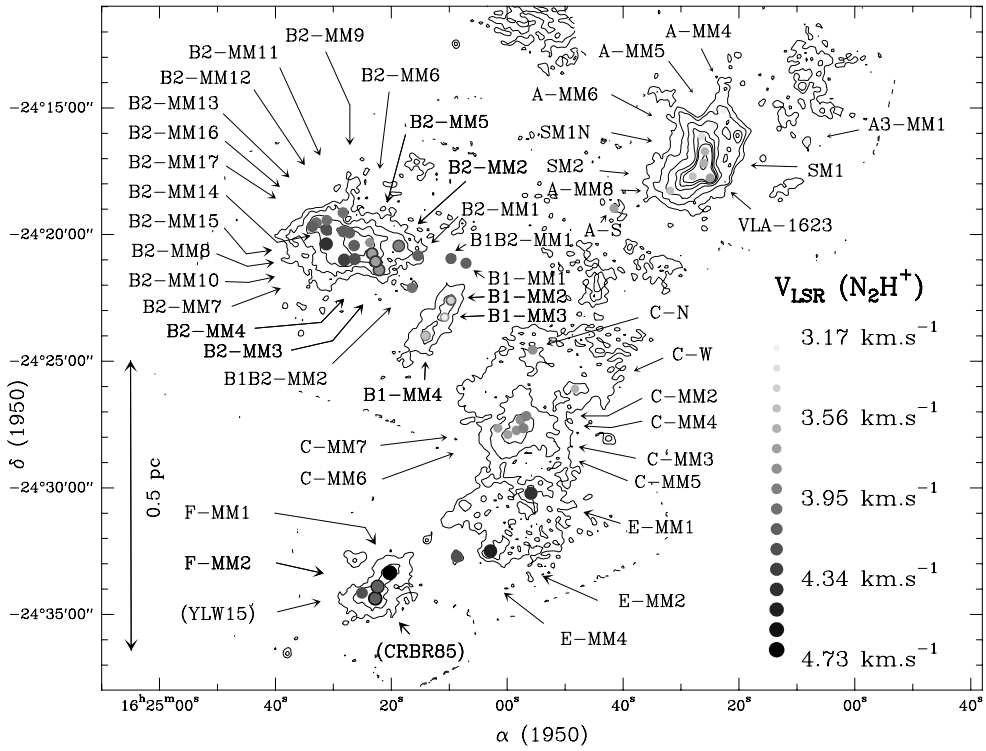

Figure 1. Line-of-sight systemic velocities of the ρ Oph protocluster condensations identified by MAN98, overlaid on the lowest contours of their 1.3mm continuum mosaic. Each condensation is represented by a filled circle whose size increases with V_{LSR}. The color coding varies from light grey to black with increasing Doppler shift. The velocities were derived from Gaussian fits to the N_2H^+(1–0) multiplet spectra.

2. New observations in molecular lines

We have carried out follow-up observations of a subsample of 54 condensations with the IRAM 30m telescope in molecular lines such as N_2H^+(1–0), C_3H_2(2–1), $H^{13}CO^+$(1–0), DCO^+(2–1), DCO^+(3–2), $H_2CO(2_{12} - 1_{11})$, CS(2–1) and CS(3–2). As an example of our results, Fig. 2b shows an $H^{13}CO^+$(1–0) integrated intensity map of the ρ Oph-E dense core obtained in the on-the-fly scanning mode. It clearly reveals the condensations OphE-MM2 and OphE-MM4 (compare Fig. 2b with the detailed 1.3 mm continuum map shown in Fig. 2a). More generally, our line observations confirm that the condensations identified by MAN98 in the continuum are real structures.

3. Linewidths of the condensations

We detected the N_2H^+(101–012) line toward 45 of the 54 condensations observed (cf. Figs. 1 and 3). The narrow linewidths we measure ($< \Delta V_{FWHM} > \sim$

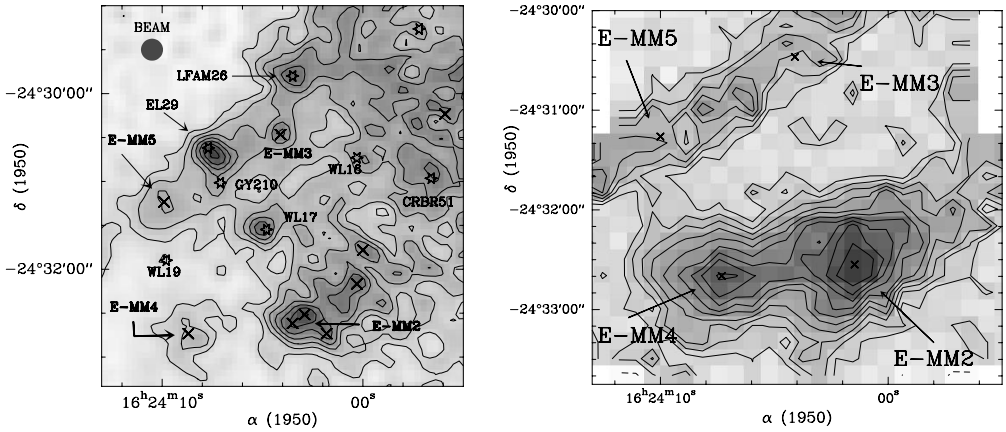

Figure 2. a) Detailed 1.3 mm continuum map of the ρ Oph-E dense core extracted from the map shown in Fig. 1 of MAN98 (13″ beam). b) Integrated $H^{13}CO^+$(1–0) intensity map of the ρ Oph-E dense core (28″ beam).

0.5 km s^{-1}) imply virial masses ($M_{vir} \sim 3 - 5 \times \frac{R\sigma^2}{G}$) less than twice the mass estimates derived from the 1.3 mm continuum in ∼ 75% of the cases. This confirms that most of the ρ Oph condensations are gravitationally bound and thus likely pre-stellar in nature.

The non-thermal velocity dispersion is about half the thermal velocity dispersion ($\frac{\sigma_{NT}}{\sigma_T} \sim 0.7$) toward the condensations of the dense cores OphB1, C, E and F. These condensations are thus characterized by small levels of turbulence, in contrast to their parent dense cores on larger scales (cf. Loren et al. 1990). This is reminiscent of models in which protocluster condensations correspond to turbulence-free zones within more massive, turbulent cores (cf. Myers 1998).

4. Relative motions of the protocluster condensations

Our line observations provide additional information about the relative motions of the condensations within the protocluster. The systemic velocities V_{LSR} of the condensations were derived from Gaussian fits to the N_2H^+(1–0) multiplet. These velocities are represented by circles in Fig. 1 overlaid on the lowest contours of the continuum map of MAN98.

A global velocity gradient of ∼ 1.2 km s^{-1} pc^{-1} is seen from North-West to South-East (see also Loren 1989 in ^{13}CO and Loren et al. 1990 in DCO^+), but the velocity differences between neighboring condensations are small. From observations of the 45 protocluster condensations detected in N_2H^+, we estimate a global one-dimensional velocity dispersion of $\sigma_{1D} \sim 0.37$ km s^{-1} about the mean systemic velocity $V_{mean} \sim 3.93$ km s^{-1}. Assuming isotropic relative motions, this corresponds to a three-dimensional velocity dispersion of only $\sigma_{3D} \sim 0.64$ km s^{-1}. With a ρ Oph main cloud diameter of ∼ 1.1 pc, such a small velocity dispersion implies a typical crossing time $D/\sigma_{3D} \sim 1.7 \times 10^6$ yr. The individual crossing times determined for the cores with a statistically sig-

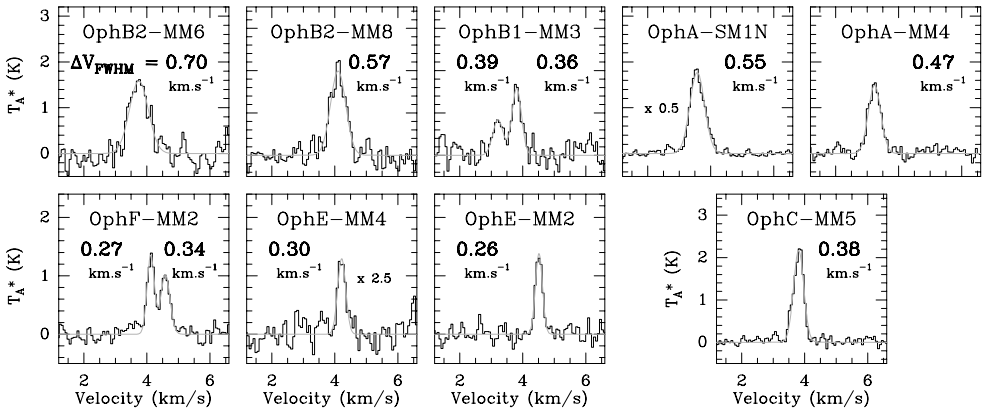

Figure 3. N_2H^+(101–012) spectra toward a subsample of ρ Oph protocluster condensations. The FWHM linewidth derived from a Gaussian fit is given in each panel.

nificant number of condensations (Oph A, B2, and C) are only slightly shorter ($\sim 0.6 \times 10^6$ yr). Since neither the age of the embedded IR cluster nor the lifetime of the 1.3 mm condensations can be much larger than 10^6 yr (e.g. Wilking et al. 1989; Bontemps et al. 2001), it appears that the pre-stellar condensations do not have time to orbit through the protocluster gas. Our ρ Oph observations therefore seem inconsistent with models which resort to the motions of the condensations/protostars within the gas to build up a mass spectrum comparable to the IMF through competitive accretion (e.g. Bonnell et al. 1997). Likewise, as pointed out by Elmegreen (2000 – see also review by Elmegreen in this volume), there is probably not enough time for the condensations to interact and collide with each other, a dynamical process which characterizes protocluster evolution in the numerical simulations of Klessen & Burkert (2000 – see also Klessen, this volume).

The above estimate of the velocity dispersion σ_{1D} among the condensations corresponds to a virial or binding mass of $\sim 53 - 88$ $M_\odot$ ($3 - 5 \times R\sigma_{1D}^2/G$), which is much less than the total gas mass ~ 550 $M_\odot$ of the ρ Oph main cloud (cf. Wilking & Lada 1983) and comparable to the total stellar mass of the present infrared embedded cluster ($M_{\rm star} \sim 100$ $M_\odot$, Bontemps et al. 2001). This comparison suggests that the ρ Oph system is gravitationally unstable and possibly in a state of overall gravitational collapse (e.g. Troland et al. 1996 – see also the asymmetric CO and ^{13}CO profiles of Encrenaz et al. 1975). It will most likely form a bound star cluster even if all the gas is removed.

5. Internal motions of the protocluster condensations

5.1. Infall

Toward at least five starless condensations (OphC-MM5, OphA-SM2, OphB2-MM16, OphE-MM2 and OphE-MM4), we observed the classical spectral signature of collapse (cf. Evans 1999, Myers et al. 2000). Optically thick tracers

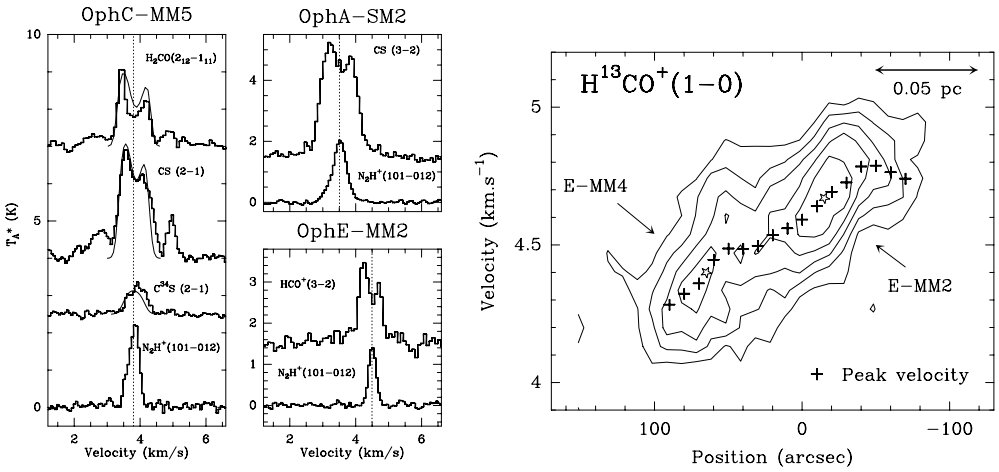

Figure 4. a) The classical spectral signature of collapse is seen toward the condensations OphC-MM5 (*left*), OphA-SM2 (*middle up*) and OphE-MM2 (*middle down*). The observations were made with the IRAM 30m telescope. See the text for the parameters of the model overlaid on OphC-MM5 spectra. b) $H^{13}CO^+(1–0)$ position-velocity diagram (*right*) along the East-West axis joining OphE-MM4 to OphE-MM2 (star markers). The crosses represent the peak velocities as determined by Gaussian fits.

such as CS(2–1), $H_2CO(2_{12} - 1_{11})$ and $HCO^+(3–2)$ show a self-absorbed line with a stronger blue peak, while thinner tracers such as $N_2H^+(101–012)$ and $C_3H_2(2–1)$ peak in the dip between the blue and red peaks (cf. Fig. 4a). This blue asymmetry appears in optically thick lines when a gradient in excitation temperature toward the center is combined with infall motions (e.g. Leung & Brown 1977).

Using a Monte Carlo radiative transfer code (Bernes 1979; Blinder 1997), we have modeled the CS(2-1), $C^{34}S$(2-1) and $H_2CO(2_{12}$-$1_{11})$ emission from the starless condensation OphC-MM5. We assumed a uniform kinetic temperature of 7 K and the density profile was constrained by the dust continuum observations of MAN98. The abundances were 2.6×10^{-10} for CS, 1.2×10^{-11} for $C^{34}S$ and 4.0×10^{-10} for H_2CO. We took an enveloppe radius of 20000 AU and an infall velocity field with a maximum value of $V_{\rm max} = 0.3$ km s^{-1} at 5000 AU. The velocity and density profiles we used are typical of the gravitational collapse of a Bonnor-Ebert isothermal sphere (Foster & Chevalier 1993). This preliminary model suggests a mass infall rate as high as $\dot{M}_{\rm inf} \sim 1 \times 10^{-4}$ M$_\odot$ yr^{-1} at $R = 5000$ AU. If confirmed, these derived infall speed and mass infall rate would be larger than those observed for the isolated pre-stellar core L1544 (e.g. Tafalla, this volume) and larger than the most extreme speed and rate that can be accounted for by ambipolar diffusion models (cf. Ciolek & Basu 2000).

5.2. Rotation

The position-velocity diagram in Fig. 4b investigates the internal kinematics of the two condensations OphE-MM4 and OphE-MM2. The $H^{13}CO^+$(1–0) peak velocities reveal two parallel but distinct velocity gradients of $\sim +7$ km.s^{-1}.pc^{-1}, centered on the position of each condensation and embedded in a larger scale gradient of $\sim +5$ km.s^{-1}.pc^{-1} . This suggests that OphE-MM2 and OphE-MM4 have started to decouple from their common parent cloud core, increasing their own spins in the process. This is in agreement with the idea that both condensations are already dynamically contracting (see the infall spectrum of OphE-MM4 in Fig. 4a).

References

André, P., Motte, F., Bacmann, A., & Belloche A. 1999, in Star Formation 1999, Ed. T. Nakamoto, Nobeyama : Nobeyama Radio Observatory, p. 145

Bernes, C. 1979, A&A, 73, 67

Blinder, S. 1997, Thesis, Université de Bordeaux I

Bonnell, I. A., Bate, M. R., Clarke, C. J., & Pringle, J.E. 1997, MNRAS, 285, 201

Bontemps, S., André, P., Kaas, A. et al. 2001, A&A, in press – see also ESA SP-427, p. 475

Ciolek, G.E., & Basu, S. 2000, ApJ, 529, 925

Elmegreen, B. 2000, in Star Formation from the Small to the Large Scale, Eds. F. Favata, A. Kaas, & A. Wilson, ESA SP-445, p. 265

Encrenaz, P.J., Falgarone, E., & Lucas, R. 1975, A&A, 44, 73

Evans, N.J., II 1999, ARA&A, 37, 311

Foster, P.N., & Chevalier, R.A. 1993, ApJ, 416, 303

Klessen, R.S., & Burkert, A. 2000, ApJS, 128, 287

Larson, R.B. 1969, MNRAS, 145, 271

Leung, C.M., & Brown, R.L. 1977, ApJ, 214, L73

Loren, R.B. 1989, ApJ, 338, 925

Loren, R.B., Wootten, A., Wilking, B.A. 1990, ApJ, 365, 229

Motte, F., André, P., & Neri, R. 1998a, A&A, 336, 150 (MAN98)

Motte, F., André, P., Neri, R., & Abergel, A. 1998b, in Star Formation with the Infrared Space Observatory, ASP Conf. Ser., 132, 163

Myers, P.C. 1998, ApJ, 469, L109

Myers, P.C., Evans, N.J., II, & Ohashi, N. 2000, in Protostars and Planets IV, Eds Manning, Boss, & Russell (Univ. of Arizona Press, Tucson), p. 217

Troland, T.H., Crutcher, R.M., Goodman, A.A., Heiles, C., Kazès, I., & Myers, P.C. 1996, ApJ, 471, 302

Whitworth, A. & Summers, D. 1985, MNRAS, 214, 1

Wilking, B.A., Lada, C.J., & Young, E.T. 1989, ApJ, 340, 823

Wilking, B.A., & Lada, C.J. 1983, ApJ, 274, 698